J Appl Electrochem (2009) 39:1617–1623
DOI 10.1007/s10800-009-9850-1

ORIGINAL PAPER

Effect of nitrate ions on the corrosion of stellite in permanganate media

Veena Subramanian · Sinu Chandran · S. Velmurugan · S. Rangarajan · S. V. Narasimhan

Received: 31 July 2008 / Accepted: 20 February 2009 / Published online: 7 March 2009
© Springer Science+Business Media B.V. 2009

Abstract The dissolution behaviour of stellite #3 in two oxidizing agents of equivalent acidity namely, permanganic acid ($HMnO_4$) and a mixture of nitric acid and potassium permanganate (NP) was evaluated. The presence of nitrate in the permanganate formulation was found to reduce its efficiency for oxidizing stellite. Electrochemical polarization and impedance studies were carried out at 90 °C in NP and $HMnO_4$. The redox potential of both the oxidizing agents favoured transpassive dissolution of chromium from the alloy. In NP, only the chromium depleted inter-phase boundary was attacked while most of the chromium rich carbide phases were intact. In contrast, in $HMnO_4$, uniform corrosion of the surface was observed. The impedance response was found to change with duration of exposure. The nitrate ions in permanganate were found to promote the repassivation of the surface. $HMnO_4$ was found to be a better formulation for dissolving cobalt from the alloy as compared to NP.

Keywords Stellite #3 · Permanganic acid · Nitric acid permanganate · Electrochemical impedance spectroscopy

1 Introduction

Stellite alloys or stellite coated surfaces are frequently used as the material of construction for the internals of valves, pumps etc., in water cooled nuclear reactor systems owing to their hardness. Under the combined effect of high-mechanical stress and the flow of coolant, the stellite surfaces corrode and the released materials may enter the core either as particles or as soluble species [1]. Subsequently they get neutron activated during circulation and are deposited preferentially in low-flow areas and in crevices existing in the coolant circuits giving rise to hotspots. As stellite alloys are rich in cobalt, the predominant radionuclide formed by neutron activation is the long-lived ^{60}Co ($t_{1/2}$ 5.27 years) isotope. Such radioactive hot spots, due to particles containing cobalt, have been observed in many nuclear reactors in the world [2]. Radioactive hotspots in a nuclear reactor amounts to excess costs as there will be an increase in the duration of shutdowns and maintenance operations.

Stellite #3 contains about 50% Co, 30% Cr, 12% W and about 2.4% C constituting about 29 wt% carbides. The resistance to aqueous corrosion critically depends on chromium as in stainless steels. However, during the formation of carbides, a good portion of chromium gets tied up with carbon making it unavailable for oxidative resistance [3]. Hence in this multi-phase alloy, the inter-phase boundaries will be depleted in chromium making it somewhat susceptible to aqueous corrosion. This factor is made use of in our study and we show that the radioactive hotspots which are mainly due to stellite particles can be eliminated by dissolving them using suitable chemical reagents.

Strong oxidizing agents such as acidified and alkaline permanganate were chosen for this purpose. Extensive studies on the dissolution of stellite #3 in the form of metallic powder have shown that acidified permanganate reagents are more efficient in dissolving chromium and cobalt from this alloy as compared to alkaline permanganate [4]. Among the acidified permanganate reagents also,

V. Subramanian · S. Chandran · S. Velmurugan · S. Rangarajan · S. V. Narasimhan (✉)
Water and Steam Chemistry Division, BARC Facilities, Kalpakkam, Tamilnadu 603102, India
e-mail: svn@igcar.gov.in

permanganic acid ($HMnO_4$, used in the CORD process) [5] has better dissolution capabilities as compared to Nitric acid Permanganate(NP) of similar acidity. It was of interest to study this aspect. The corrosion behavior of the alloy in these chemical reagents was expected to give an insight into the differences in their oxidizing capabilities and hence dissolution efficiency. Hence in this study, electrochemical techniques were used to measure their corrosion rates. This paper gives a brief account of attempts to understand the reaction mechanisms involved in the corrosion process using electrochemical impedance spectroscopy (EIS) and polarization techniques. Surface analytical techniques like SEM/EDX and XPS were used to support EIS data.

2 Experimental

All the solutions were prepared using AR grade reagents. A stock solution of ~8 mM $HMnO_4$ was prepared by passing appropriate concentration of $KMnO_4$ solution through H^+ form of cation exchange resin. Solutions of Nitric acid-permanganate (NP) were prepared by mixing appropriate quantities of potassium permanganate ($KMnO_4$) and Nitric acid in double distilled water and making up to 1 L. The concentrations used for all the experiments were 2.5 mM of $HMnO_4$ and for NP, it was a mixture of 2.5 mM nitric acid and 2.5 mM $KMnO_4$, so as to maintain same acidity in both the solutions.

Electrochemical studies were made using Eco Chemie Autolab PG STAT30 system. The stellite discs of 0.29 cm^2 area were mounted in PTFE blocks and polished up to 1000 grit silicon carbide papers, and later using 2 μm diamond paste. A three-electrode configuration was used with platinum foil as counter electrode and the potential was measured using a saturated calomel electrode as the reference that was connected through a luggin capillary. For EIS measurements, a 10 mV excitation signal was applied and the frequency was scanned from 10 kHz to 5 mHz. For potentiodynamic polarization methods, the scan rate was fixed at 0.5 mV s^{-1}. The XPS studies were carried out on stellite coupons using VG ESCA-Lab equipment. Scanning electron micrographs were taken by using a PHILLIPS ESEM XL-30 system.

3 Results and discussions

3.1 Powder dissolution

A three step 3 cycle redox process was adopted for dissolving stellite #3 powder of particle size ranging from 70 to 250 μm. The first step was the oxidation step, in which the chromium present in the stellite was oxidized using a permanganate based reagent by exposing it for 24 h. In the second step, the unreacted permanganate and the reaction product MnO_2 was decomposed by adding adequate quantity of citric acid. The third step involved treatment with a reducing agent comprising a solution containing EDTA, ascorbic acid and citric acid (EAC), in the weight ratio 4:3:3. Temperature was maintained at 90 °C during the whole process. Dissolution of cobalt from stellite was observed to start during the citric acid step and continued till the EAC step. The solution was analyzed periodically for cobalt and chromium using Atomic Absorption Spectrometry (AAS). Figure 1 gives the percentage dissolution of chromium and cobalt at 90 °C in a single oxidation—reduction step. In effect, stellite #3 could be dissolved to the extent of ~40% by using $HMnO_4$ as the oxidizing agent and EAC as the reducing agent in a single redox cycle. However, complete dissolution of stellite was achieved by repeating the redox process in 3 consecutive cycles. On the other hand, in NP/CA/EAC reagents only about 5% of the alloy could be dissolved in a single redox cycle.

3.2 Surface characterization

Stellite #3 was etched with an etchant (100 mL HCl mixed with 0.5 mL of 30% H_2O_2) to observe its microstructure [6]. A SEM micrograph of an etched specimen is given in Fig. 2. It shows carbide phase (chromium rich) dispersed in a matrix phase which has cobalt as the major element. The tungsten rich carbide phases appear brightest in the BSE image. The composition of each phase is given in Table 1 as measured by energy dispersive X-ray microanalysis (EDX).

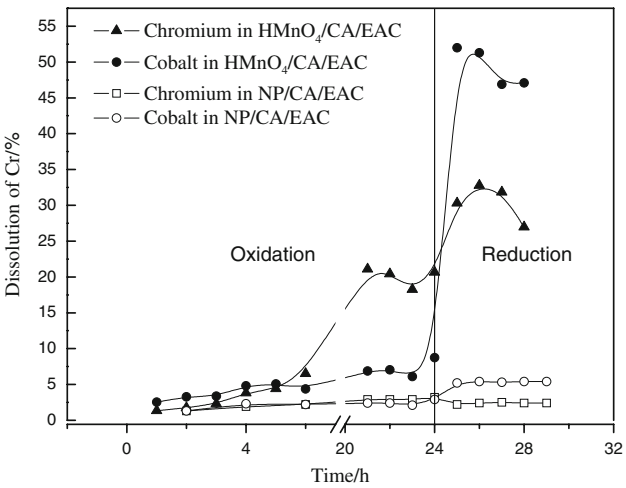

Fig. 1 Extent of Cr and Co dissolution from stellite in a single redox cycle at 90 °C

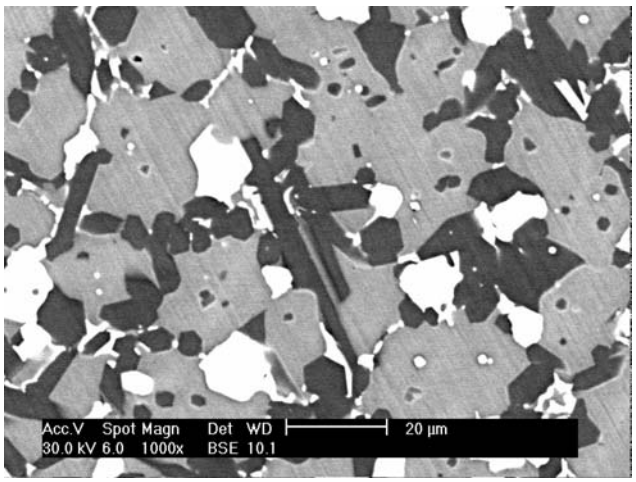

Fig. 2 Microstructure of stellite #3

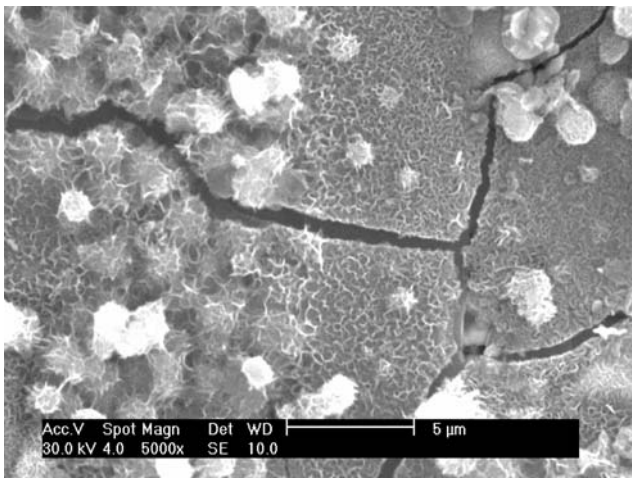

Fig. 3 Stellite #3 in $HMnO_4$ for a shorter duration of exposure

Table 1 The composition of different phases

Phase	Co/wt%	Cr/wt%	W/wt%	Fe/wt%
Matrix	68.1	18.58	9.58	3.76
Carbide phase	19.7	68	11.3	1.1
W-phase	28.3	14.9	53	1.8

In order to observe the change in surface morphology during the course of time, two set of experiments were carried out. In one, the alloy was exposed to the two oxidizing solutions at 90 °C for a shorter duration of 50 min, so that the system was stabilized with respect to its OCP, and the specimens were taken out and characterized using SEM/EDX and XPS. In the other, the specimens were exposed to a full redox cycle using NP, as well as $HMnO_4$, and were also analyzed using the above mentioned surface techniques.

The stellite #3 specimen exposed to $HMnO_4$ for 50 min was observed to have a thin chromium containing film on the surface (Fig. 3). The film was broken at some places. Dark and bright particles that were present on the specimen were found to be rich in cobalt (~60%), the brighter ones containing more Mn (~11%) than the darker ones (3.8%). XPS analysis showed traces of cobalt as Co_3O_4. Figure 4 gives the XPS spectra of Manganese, Chromium and tungsten for this specimen. Mn $2p_{3/2}$ peak was quite broad with a FWHM of 3.72 eV, with a peak position of 641.4 eV indicating a mixture of Mn_2O_3 and MnO_2. Cr was present more in its Cr_2O_3 form and to a lesser extent in its metallic form. Tungsten was mostly present as WO_3 and a feeble peak corresponding to metallic W also was observed. Oxygen peak (not shown in Fig. 4) indicated transition metal oxides and OH (adsorbed water).

SEM micrographs of Stellite #3 exposed to NP for short duration did not show a film on the surface (Fig. 5). It also

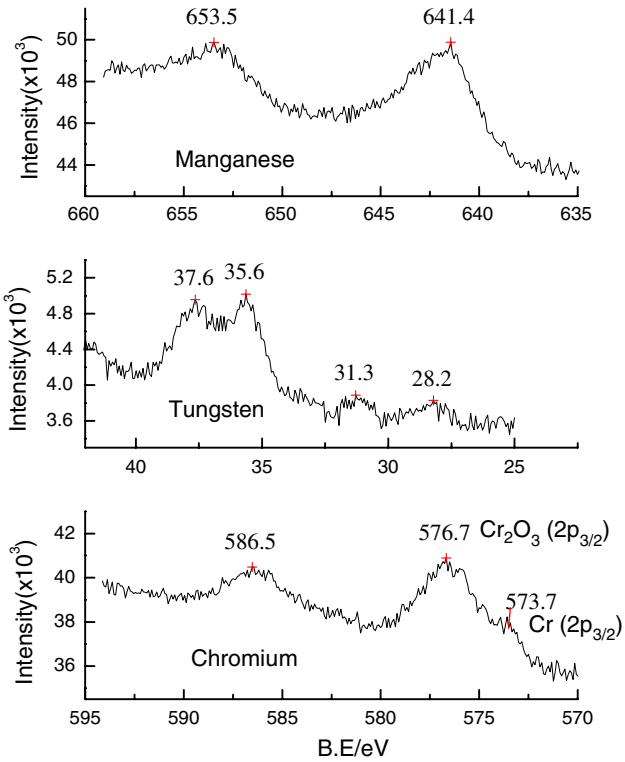

Fig. 4 XPS spectra for stellite #3 exposed to $HMnO_4$ for 50 min

showed many deep pits on Co rich matrix phases (not seen in this figure). The micrograph clearly showed different phases present in the alloy. It could be observed from the secondary electron image that some phases were more elevated than the others. The phase that was preferentially corroding (corresponding to lesser elevated regions) was found to be rich in Cobalt (about ~67% Co) as analyzed by EDX. The other rod like structured phase was rich in Chromium (~67%) and the brightest phase in the SE image corresponded to tungsten-rich phase (~60%). This

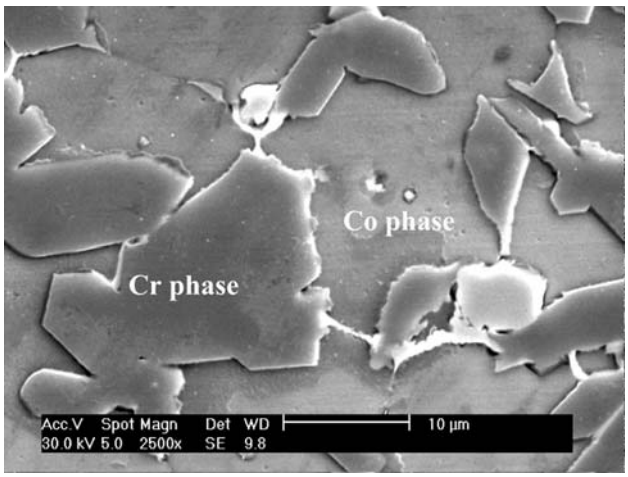

Fig. 5 Stellite #3 in NP for a shorter duration of exposure

short exposure to NP revealed the microstructure of the alloy. The Cr-depleted regions at the edges of carbide phases were also visible in this picture. The main difference in the XPS spectrum of this specimen with that exposed to $HMnO_4$ for a shorter duration was that cobalt was not present on the surface (Fig. 6).

Figure 7 shows the specimen subjected to a full redox cycle with $HMnO_4$ as oxidizing agent (i.e., $HMnO_4$ for 24 h, Citric acid for 1 h and EAC for 3 h). The markings 1, 2, and 3 correspond to cobalt-rich, chromium-rich and tungsten-rich phases respectively. Severe corrosion especially in the inter-phase boundaries was observed. Shallow pits were seen on cobalt rich phase but the rod like Cr-rich phase had no pits. XPS analysis indicated that both cobalt and manganese were absent from the surface. Chromium and Tungsten were mostly present as their oxides Cr_2O_3 and WO_3 but traces of their respective metallic

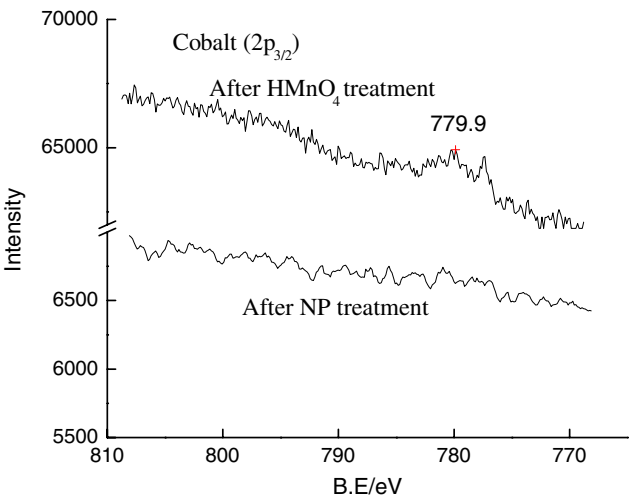

Fig. 6 XPS spectra of Cobalt for stellite #3 exposed to $HMnO_4$ and NP for 50 min

counterparts were also seen. The oxygen peak indicated the presence of both oxy-hydroxide and oxides. Similarly, the specimen which had undergone a full redox cycle with NP as oxidizing agent showed deep pits on the cobalt phase and the surface appeared less attacked with a less corrosion at the inter-phase boundaries and very intact chromium phases (Fig. 8).

The main difference between the actions of the two oxidizing agents as observed by the surface analytical techniques may be listed as follows. Corrosion takes place more or less uniformly in $HMnO_4$ and hence the surface morphology shows broken carbides and reduced area fractions for all the phases after the completion of one redox step. From XPS and SEM analysis it may be concluded that both cobalt and chromium gets oxidized to form a thin film. However, this film was found to broken and hence not protective. But in the NP/stellite system, corrosion took place mainly on chromium depleted regions. An initial treatment with NP leaves behind a cobalt depleted and hence chromium-rich surface as shown by XPS. This chromium rich surface is not further oxidised by NP.

3.3 EIS measurements at 90 °C with increase in exposure time

Electrochemical impedance measurement was done after the stabilization of the open circuit potential for 50 min and is referred to here as 0th h spectra. Figure 9 shows the 0th h impedance spectra in NP and in $HMnO_4$ which indicates the presence of at least one capacitive and one inductive time constants. In both the media the spectra showed a prominent inductive loop at lower frequencies implying reaction occurring through a soluble intermediate [7]. This type of impedance response has been associated with transpassive dissolution of chromium in various chromium containing alloys [8–10].

At the film-solution interface, the active reactant MnO_4^- is adsorbed onto the surface film and oxidizes Cr(III) to its more soluble form i.e., Cr(VI) and in turn is reduced to MnO_2. This involves a $3e^-$ transfer from the reactant. Due to the oxidation of the underlying metal a Cr_2O_3 film grows in situ at the metal/film interface. The kinetics of oxidation of Cr(0) are relatively fast and hence the reaction at the film/solution interface is rate determining. The physical model for the interfacial reactions can be described as given in Fig. 10.

An oxide of Cr(III) probably forms a soluble intermediate in this whole process of oxidation-dissolution. There exists at least two multiple e^- transfer processes at the interface leading to an inductive type of response. During oxidation, most of the cobalt is retained on the surface.

Based on this physical model, the impedance spectra were fitted to an electrical equivalent circuit as shown in

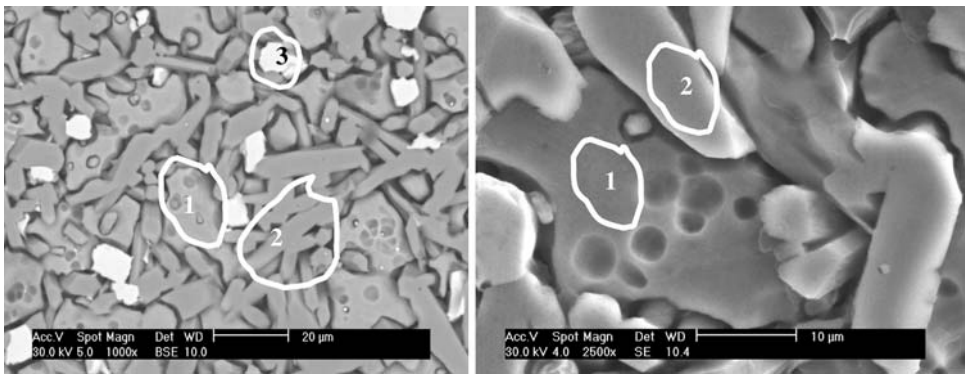

Fig. 7 Stellite #3 after $HMnO_4$/CA/EAC (duration of exposure = 28 h)

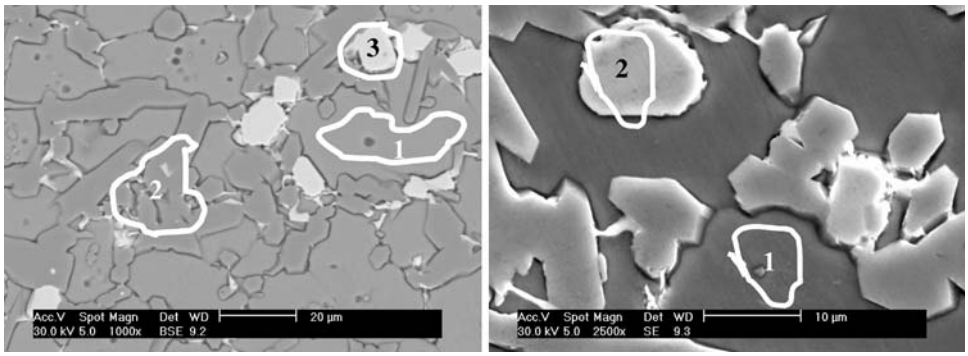

Fig. 8 Stellite #3 after NP/CA/EAC (duration of exposure = 28 h)

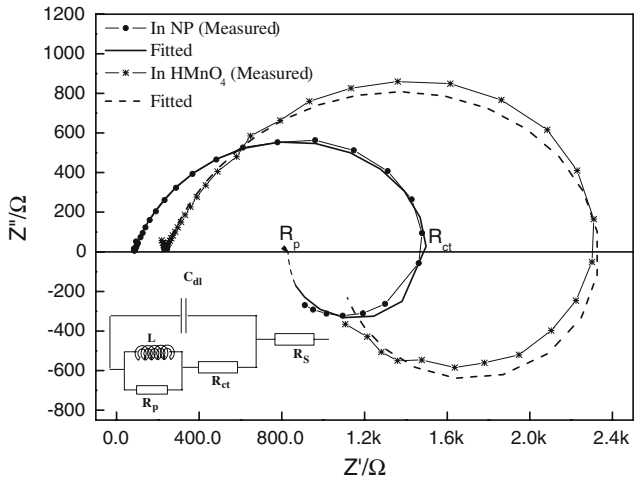

Fig. 9 Impedance spectra for stellite #3 in $HMnO_4$ and NP at 90 °C

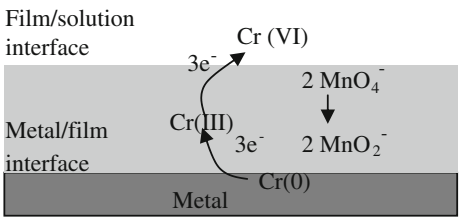

Fig. 10 Physical model depicting reactions at the interfaces

Fig. 9. The two resistances R_{ct} and R_p in series arise due to the two step oxidation process of chromium which are inter-dependent.

Figure 11 shows impedance measurements for stellite #3 in $HMnO_4$ as a function of time. Up to about 5 h there was a gradual increase in the absolute impedance values which later decreased abruptly and remained constant till 24 h. Citric acid was added to the same solution to decompose the reaction product MnO_2 and the unreacted excess $HMnO_4$. Subsequent to the addition of citric acid (to remove MnO_2 and excess $HMnO_4$), the impedance response was found to change to that indicating mixed control involving charge transfer and diffusional impedance. In the reduction step with EAC, the rate was observed to be highly time dependent and the Nyquist plot indicated a system which has not yet reached a steady state.

However in the case of NP, the inductive loop completely disappeared after about 10 h of exposure (Fig. 12a). The disappearance of the inductive loop in NP after about 10 h suggests that at least one of the Faradaic steps is hindered during the course of the reaction. One reason may be the change in activation energy because of the modification of the surface during the course of the reaction. Passivation of the surface is also reflected in the absolute impedance values of 350–400 kΩ in the reduction step (Fig. 12b).

Figure 13 gives the variation of charge transfer resistances observed for stellite 3 in both the oxidants and the

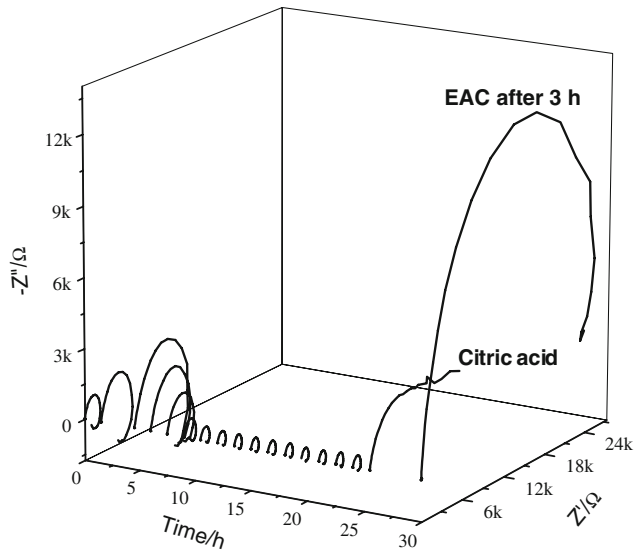

Fig. 11 Impedance spectra with time for stellite #3 in one redox step using $HMnO_4$, CA and EAC

inset in Fig. 13 gives the corresponding change in the open circuit potentials (OCP) measured versus SCE. Initially with $HMnO_4$, the value of absolute impedance decreases gradually for about 5 h and then starts increasing and reaches a steady state after about 10 h. This coincides with the gradual increase in OCP after ~5 h. As the process of corrosion involves a change in valency of chromium, it is strongly dependent on potential. Hence a marginal change of ~20 mV in potential increases the rate of transpassive dissolution of chromium. This sudden change in the system may be due to breakdown of passivity of the alloy. In our previous study [4], the XPS spectra for stellite #3 exhibited chromium in both metallic, as well as in Cr_2O_3, form, while the cobalt was mostly present in its metallic form. Based on a calculation of escape depth for chromium through a Cr_2O_3 layer, the chromium signals can be obtained only if the thickness of the film is less than 3.3 nm [11]. This implies that the thickness of the barrier film on stellite #3 surface should be much less than 50 A°. In the presence of highly oxidizing anions like MnO_4^-, it is quite probable that the rate of growth of Cr- oxide film and its dissolution can not reach a steady state. This may result in break down of the passive film by a similar phenomenon by which passivity breakdown occurs in stainless steel [12]. SEM micrographs (Fig. 3) for $HMnO_4$/stellite also showed a film that has developed ~1 μm cracks. The total rate of metal loss from stellite was calculated by analyzing for chromium in the solution at the end of the experiment and it was found to be 0.0386 μm h^{-1}. This amounts a total thickness loss of 0.93 μm in 24 h, which implies that the bare metal might have been exposed during the course of the reaction.

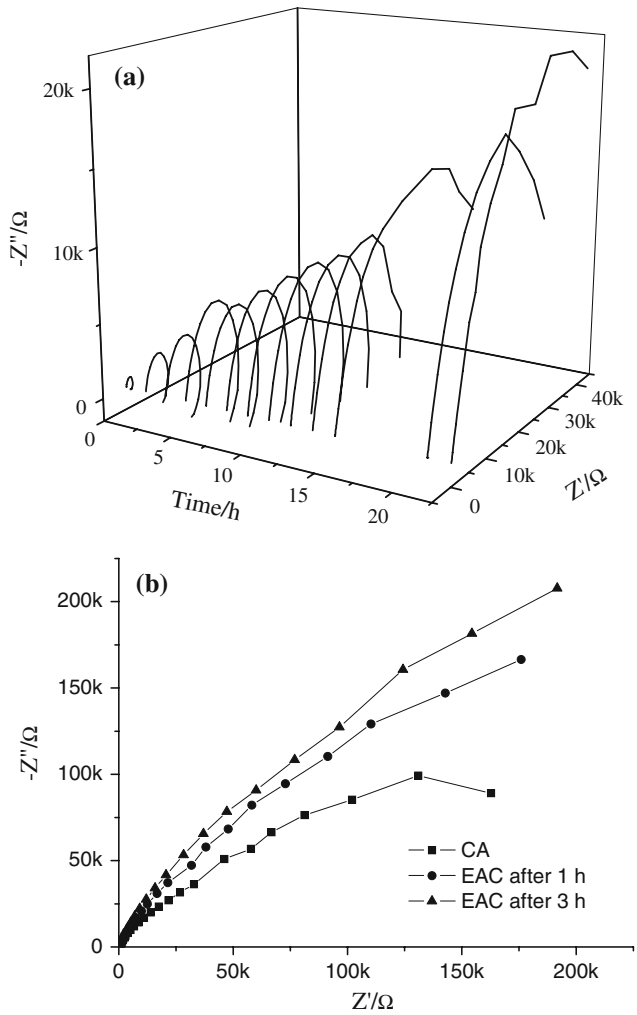

Fig. 12 Impedance spectra with time for stellite #3 in **a** NP and **b** CA and EAC at 90 °C

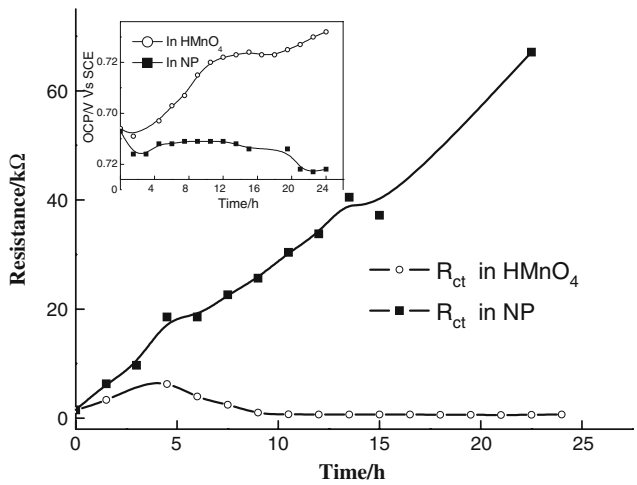

Fig. 13 Variation of charge transfer resistance with time in the case of stellite #3

On the other hand, in NP/stellite system, the OCP, after an initial drop, remains almost constant throughout the oxidation step. Here also aggressive anions are present but along with a passivator in the form of nitrate ions. This not only leads to a slow, inhibited oxidation but also promotes some form of repassivation. This was evident in the monotonic increase in R_{ct} values.

Comparison of polarization data at 0 h and after 2 h (Fig. 14) for stellite 3 in both the oxidizing agents indicated that the difference was mainly due to the cathodic reaction kinetics. The major oxidation reaction here is that of chromium and the cathodic reactions, in addition to the hydrogen evolution reaction and oxygen reduction reactions, include the reduction of MnO_4^- species (Eq. 1)

$$MnO_4^- + 4H^+ + 3e^- \rightarrow MnO_2 + 2H_2O \quad (1)$$

Only the acidity of the medium controls the rate of this reaction. However, the presence of nitrate ions during the initial stages increases the corrosion rate slightly as it provides an additional pathway for reduction in addition to Eq. 1. Further changes observed in cathodic and anodic currents during the course of time may only be attributed to the difference in surface activation. Table 2 gives the corrosion rate of stellite #3 calculated from Fig. 14 using Tafel extrapolation. In the case of NP the corrosion rate decreased by 100 times, supporting the repassivation phenomena that was observed in the impedance measurements.

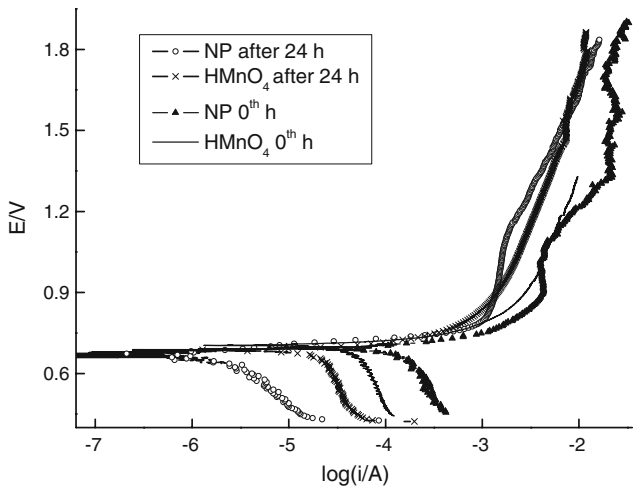

Fig. 14 Polarization curves for stellite #3 at 90 °C after 24 h exposure in $HMnO_4$ and NP

Table 2 Comparison of corrosion rates of stellite in $HMnO_4$ and NP

	$HMnO_4$		*NP*	
	0 h	24 h	0 h	24 h
Corrosion rate/mpy	20.94	12.78	46.24	0.46

4 Conclusions

The dissolution of metallic powder of stellite #3 can be best achieved by a three step redox process that involves $HMnO_4$, citric acid and EAC as reagents. Nitric acid containing permanganate with H^+ to the same extent and with the same oxidizing anionic species viz. MnO_4^- was found to be less effective in oxidizing these metallic particles. In $HMnO_4$ pretreatment, stellite #3 corrodes uniformly with a slow but constant rate during which both cobalt and chromium are oxidized. Most of the cobalt is retained on the surface, probably as Co_3O_4. EIS data also show almost a constant rate corresponding to transpassive dissolution of chromium from the alloy, after an initial hindrance due to the formation of an unstable chromium rich film. During NP/CA/EAC treatment mainly the chromium depleted regions of the alloy are attacked. Electrochemical impedance studies, along with surface characterization, indicated a repassivated surface in the presence of nitrate ions. Oxidizing pre-treatment with NP and with $HMnO_4$ results in different surface morphology. As a result the efficiency of reducing agents like citric acid and EAC for dissolving cobalt from their surfaces also falls. Further study in the direction of identifying intermediates in both the cases is required for complete understanding of the process.

References

1. Lemaire E, Le Calvar M (2001) Wear 249:338
2. Rocher A, Ridoux P, Anthoni S, Brun C (1998) Programme to eradicate hot spots (Co-60) carried out in French PWR units. 1st EC/ISOE workshop on occupational exposure management at NPPS, Malmö, Sweden, 16–18 September 1998
3. Crook P, Silence WL (2000) In: Winston Revie R (ed) Uhlig's corrosion handbook, 2nd edn. John Wiley and Sons, New York
4. Subramanian V, Chandramohan P, Srinivasan MP, Sukumar AA, Raju VS, Velmurugan S, Narasimhan SV (2004) J Nucl Mater 334:169
5. Segal MG, Swan T (1983) In: Water chemistry of nuclear reactor systems 3, vol 1. BNES, London, p 141
6. Standard practice for micro etching metals and alloys, ASTM E407-99 (1999) West Conshohocken, PA. doi:10.1520/E0407-07
7. Armstrong RD, Bell NF (1974) J Electroanal Chem 55:201
8. Bojinov M, Fabricius G, Kinnunen P, Laitinen T, Makela K, Sarrio T, Sundholm G (2000) Electrochim Acta 45(17):2791
9. Bojinov M, Fabricius G, Kinnunen P, Laitinen T, Makela K, Sarrio T, Sundholm G, Yliniemi K (2002) Electrochim Acta 47(11): 1697
10. Montero-Ocampo C, Latanision RM (1998) In: Proceedings of the symposium on passivity and breakdown. Electrochemical Society, p 308
11. Cumpson PJ, Seah MP (1998) Surf Interface Anal 25(6):430
12. Zhang Y, Macdonald DD (2006) Corros Sci 48:3812